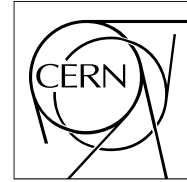




The Compact Muon Solenoid Experiment

CMS Performance Note

Mailing address: CMS CERN, CH-1211 GENEVA 23, Switzerland



13 July 2024 (v3, 14 July 2024)

Tracking performance using Tag and Probe with $Z \rightarrow \mu^+ \mu^-$ in 2022 and 2023

The CMS Collaboration

Abstract

The determination of the detector efficiency is a critical ingredient in any physics measurement. It can be in general estimated using simulations, but simulations need to be calibrated with data. The tag-and-probe method provides a useful and elegant mechanism for extracting efficiencies directly from data. In this work, we present the tracking performance measured in data where the tag-and-probe technique was applied to the Z boson resonance for all reconstructed muon trajectories and the subset of trajectories in which the CMS Tracker is used to seed the measurement. The performance is assessed using LHC 2022 and 2023 Run 3 data at 13.6 TeV.

CMS

Tracking performance using Tag and Probe with $Z \rightarrow \mu^+ \mu^-$ in 2022 and 2023

The CMS Collaboration

Contact: cms-phys-conveners-trk@cern.ch

The offline iterative tracking in CMS

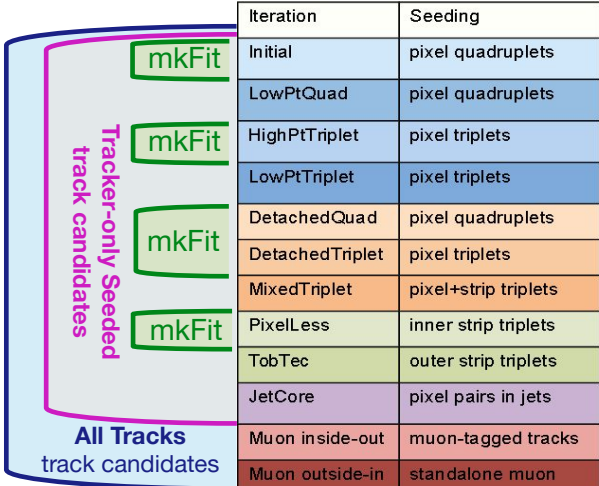
The iterative tracking approach runs a **standard Kalman Filter algorithm** multiple times. In each iteration, the hits used in previous iterations are removed and the Kalman Filter algorithm is run again with progressively looser settings [1]. The **mkFit algorithm**, implemented in CMS from 2022 data taking onwards, has been added in some tracking iterations (table in this page), and revolutionizes track pattern recognition by leveraging parallelization and vectorization on multi-core CPUs. This approach enhances computational efficiency while maintaining robust physics performance [2].

The first set of iterations are seeded by hits in the **inner tracker only**, while the last two steps listed below use **muon candidates** from the muon system to create seeds for the track reconstruction in the inner tracker.

Tracker-only Seeded track collection consists of tracks that make use of only tracker hits for the seeding.

All-Tracks collection combines the tracker-only seeded tracks with tracks which exploit the presence of muon candidates in the muon system to seed the track reconstruction in the inner tracker:

1. An **outside-in track** reconstruction step seeded in the muon system (p_T threshold 2 GeV).
2. An **inside-out iteration** that re-reconstructs muon-tagged tracks (p_T threshold 10 GeV).



Iteration	Seeding
Initial	pixel quadruplets
LowPtQuad	pixel quadruplets
HighPTTriplet	pixel triplets
LowPTriplet	pixel triplets
DetachedQuad	pixel quadruplets
DetachedTriplet	pixel triplets
MixedTriplet	pixel+strip triplets
PixelLess	inner strip triplets
TobTec	outer strip triplets
JetCore	pixel pairs in jets
Muon inside-out	muon-tagged tracks
Muon outside-in	standalone muon

The Tag and Probe method for Muon Tracking Efficiency

The tag and probe method [3] is used to extract muon tracking efficiency from data using di-muon resonances.

- **Define Probes:** Select muons using looser criteria.
- **Classify Probes:** Separate into passing and failing based on stricter criteria.
- **Define Tags:** Apply very tight selection for tag muons.
- **Pairing:** Form di-muon pairs with invariant mass near Z resonance and zero total charge ($\Delta Q = 0$).
 - Use the highest p_T valid tag-probe pair if multiple probes match a tag.
 - Exclude pairs where muons can interchange roles.
- **Efficiency (ϵ) Calculation:**
 - Background subtraction for passing and failing probes using simultaneous Fit Procedure (page 7).
 - Efficiency is the fraction of pairs with probe passing tighter selection.
- **Fake matching rate [1]:**
 - Before probes classification, measured by removing tracks combining with tags near Z boson mass (40-200 GeV).

The selections strategy

The tag-probe pairs selection process has been summarised in the flowchart on the right hand-side. More details are given below.

The tag muon

- Tight muon ID [4] with transverse momentum p_T larger than 27 GeV
- Relative combined isolation with $\Delta\beta$ correction [4] in $\Delta R = 0.4$ is applied to be less than 0.15.
- Geometrically matched to a trigger object that fired the single muon trigger for isolated muons with a nominal p_T threshold of 24 GeV.

The probe muon

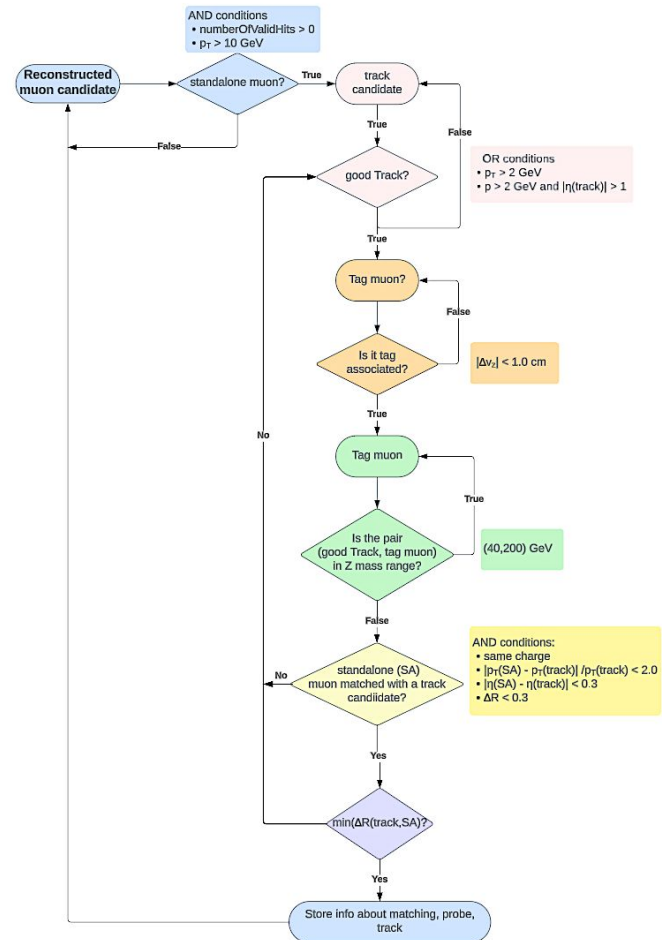
- Any standalone muon updated at vertex with more than one hit and more than one station in the muon system (i.e. good track-hit χ^2).

Passing probe criteria

- The standalone muon track at its impact parameter is matched in ($\Delta Q = 0$, $\Delta R < 0.3$, $\Delta\eta < 0.3$, $\Delta p_T/p_T(\text{probe}) < 2.0$) with minimum ΔR track (from **allTracks** or **Tracker-only seeded tracks** collection) having $p_T > 2$ GeV and $p > 2$ GeV or $|\eta| < 1$ and are associated at least with a tag in the event (difference in the vertex z-coordinate Δv_z between the two objects is less than 1.0 cm).
- The passing tag-probe mass is computed using the tracker momentum in both tag and probe to improve mass resolution.

Cuts for Tag and Probe pairs

- Select a pair of opposite-sign tag-and-probe objects.
- Z mass window for fit procedure: [70-115 GeV].



Challenges and Control Measure

Measuring tracking efficiency involves matching tracks between the inner tracker and the muon system, presenting two main challenges that must be controlled:

- **Underestimation Risk:**
 - Inner tracker track not associated with standalone muon.
 - Mitigate with loose matching criteria.
- **Overestimation Risk:**
 - Standalone muon associated with spurious tracker track.
 - Worsens with looser matching criteria, need to compute matching fake rate (*).

ϵ : measured efficiency

$\epsilon_M^{(**)}$: matching efficiency

ϵ_T : true tracking efficiency

ϵ_F : fake matching rate

$$\epsilon = \epsilon_T \epsilon_M + (1 - \epsilon_T \epsilon_M) \epsilon_F \longrightarrow 1 - \epsilon_T \epsilon_M = \frac{1 - \epsilon}{1 - \epsilon_F}$$

$$(1) \quad \Delta(\epsilon_T \epsilon_M)_{up} = \frac{(\epsilon + \sigma_{up}(\epsilon))}{1 - (\epsilon_F - \sigma_{down}(\epsilon_F))} - \epsilon$$

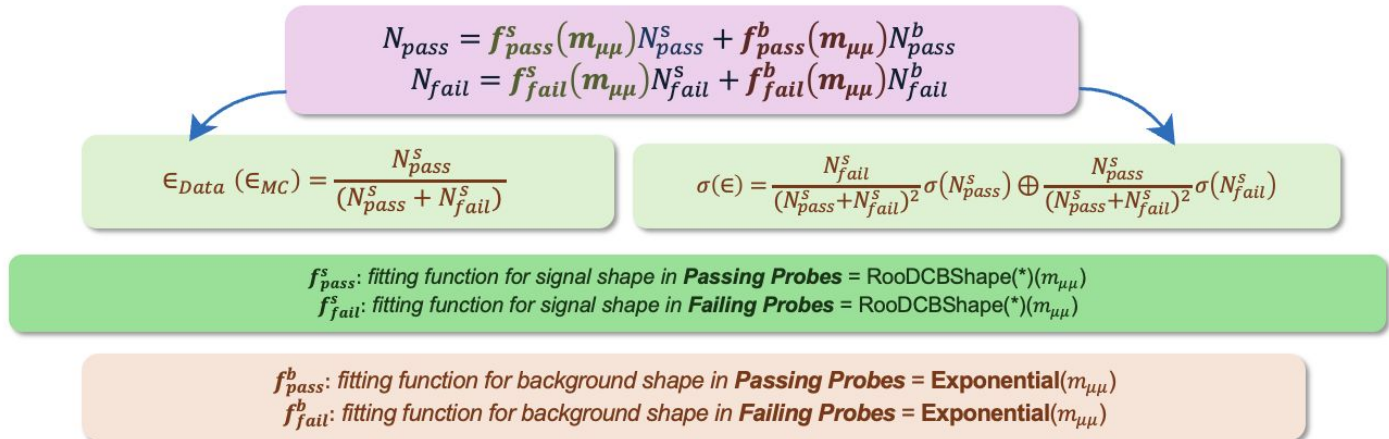
$$(2) \quad \Delta(\epsilon_T \epsilon_M)_{down} = \epsilon - \frac{(\epsilon - \sigma_{down}(\epsilon)) - (\epsilon_F + \sigma_{up}(\epsilon_F))}{1 - (\epsilon_F + \sigma_{up}(\epsilon_F))}$$

(*) $1 - \epsilon_F$ is typically around 0.9-0.95 in the sample used in this study.

(**) $1 - \epsilon_M$ is estimated to be below 0.1% except for high p_T standalone muon bins (page 11). We neglect it in the following and consider it an additional systematic uncertainty.

Fit procedure

As the **selected events** may not come from the dilepton resonance, there could be a **bias** in the efficiency measurement. To avoid this, a **simultaneous fit** to the signal and the background tag-probe invariant mass is performed (for both **passing** and **failing** probes, **data** and **MC**). This process has been repeated for each kinematic variable bin for which the measured efficiency will be provided later. The passing tag-probe mass is computed using the tracker momentum for both tag and probe.



(*) Double Sided Crystal Ball shape

Samples

In this study, the luminosity validated for physics analysis corresponding to data recorded with all detectors and reconstructed physics objects showing good performance is used. Events are passing a trigger requiring at least one muon. The selection criteria for vertices requires the presence of at least one valid vertex, with degrees of freedom greater than or equal to five. Additionally, the vertex z-position must be within ± 25 cm, and the transverse distance from the z-axis must be less than 2 cm.

2022 and 2023 Collision Certified Data in CMS

In 2022 and 2023, proton-proton collisions at a center-of-mass-energy of 13.6 TeV were recorded respectively from **5th July to 28th November 2022** and **21st April to 16th July 2023** [5]. In 2023, the data collection period is divided into two segments due to an extended LHC downtime from **13th June to 1st July**. In the second period (**2023postBPix**), readout issues were observed in the barrel pixel tracker [6], specifically in layers 3 and 4 in the same sector along the beamline, affecting track coverage within $-1.5 < \eta < -0.2$ and $-1.1 < \phi < -0.9$. Dedicated Monte Carlo (MC) samples are used to simulate each period.

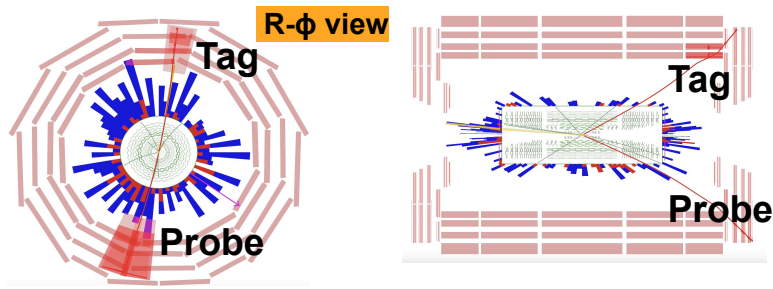
Monte Carlo Simulations

The simulations used in this study include Drell-Yan to two leptons (with invariant mass greater than 50 GeV), generated using Madgraph [7] with Tune CP5 for the underlying event. The MC distributions are reweighted to match the number of reconstructed vertices in the data. Track kinematic variables (p_T, η) are shown post-reweighting, with distinct weights applied for passing and failing probes.

$pp \rightarrow (Z \rightarrow \mu^+\mu^-) + \text{jets}$

CMS Experiment at LHC CERN 2022 (pp, 13.6 TeV)
Run/Event: 359806/722736106
Lumi section: 374

Event display is created by using FireWorksWeb [8]



R-z view

Jets

Muons

PrimaryVertices

Electrons

Example of fit (Data)

efficiency = $(98.79 \pm 0.01) \%$

$\chi^2/ndof$ pass: 12.982, fail: 2.686

--- parameters

Passing Probes

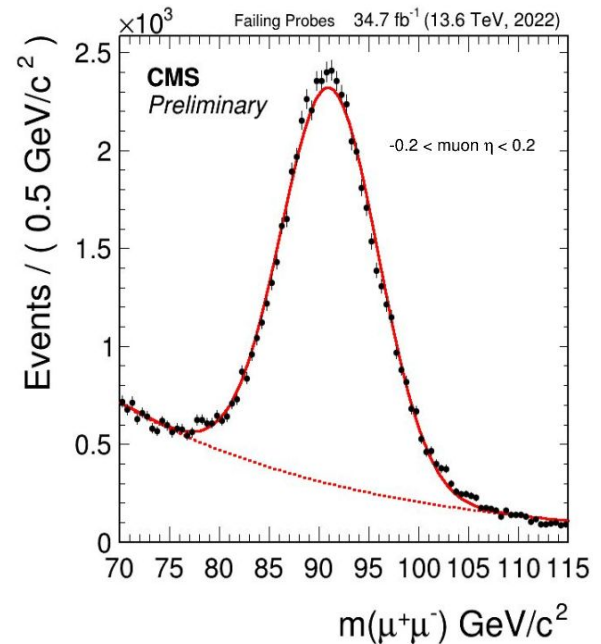
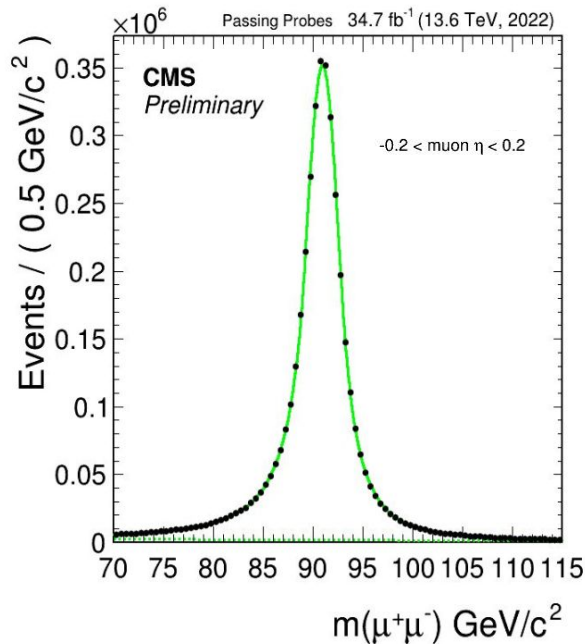
- $nBkgP = (156.01 \pm 2.99) \times 10^3$

- $nSigP = (4046.16 \pm 3.59) \times 10^3$

Failing Probes

- $nBkgF = (29.11 \pm 0.21) \times 10^3$

- $nSigF = (49.51 \pm 0.25) \times 10^3$



The fit in **Passing** and **Failing Probes** plots for the **pseudorapidity η probe** bin $[-0.2, +0.2]$ as a function of the invariant mass of the Tag and Probe muons in the **Tracker-only Seeded tracks** collection. Data are shown in black dots. The **Passing** tag-probe mass is computed using the tracker momentum for both tag and probe, improving the mass resolution.

Example of fit (MC)

efficiency = $(99.38 \pm 0.01) \%$

χ^2/ndof pass: 8.260, fail: 1.530

--- parameters

Passing Probes

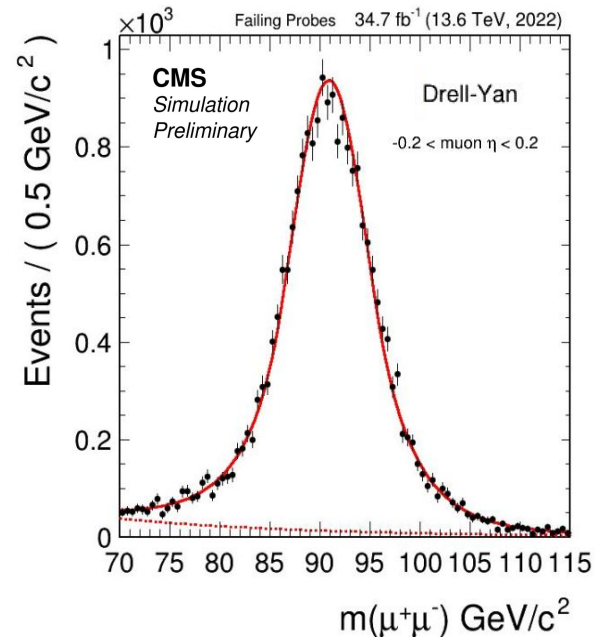
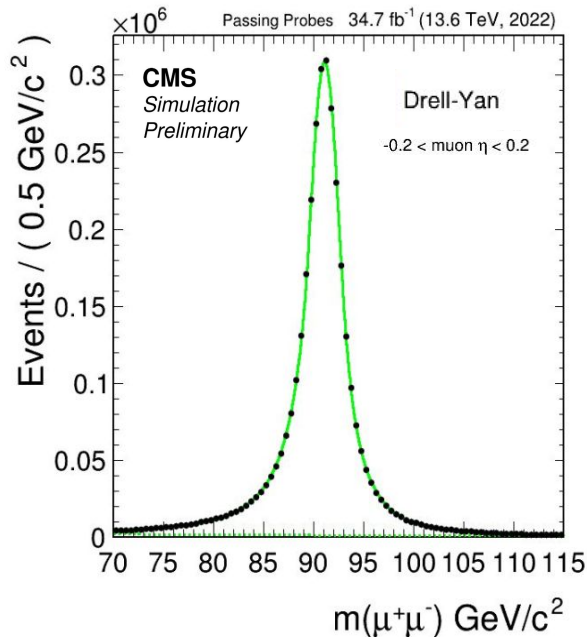
- $n\text{BkgP} = (117.66 \pm 2.30) \times 10^3$

- $n\text{SigP} = (3399.07 \pm 2.92) \times 10^3$

Failing Probes

- $n\text{BkgF} = (1.34 \pm 0.24) \times 10^3$

- $n\text{SigF} = (21.32 \pm 0.28) \times 10^3$



The fit in **Passing** and **Failing Probes** plots for the **pseudorapidity η probe** bin $[-0.2, +0.2]$ as a function of the invariant mass of the Tag and Probe muons in the **Tracker-only Seeded tracks** collection. Drell-Yan MC is shown in black dots. The **Passing** tag-probe mass is computed using the tracker momentum for both tag and probe, improving the mass resolution.

2022 Track kinematics

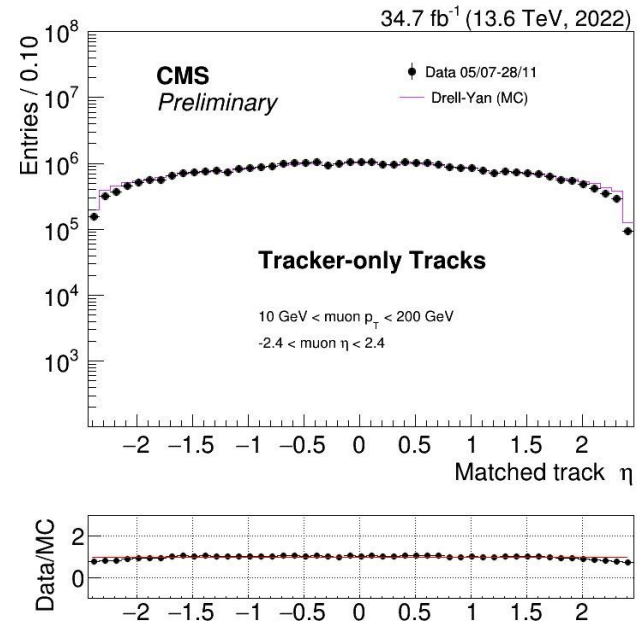
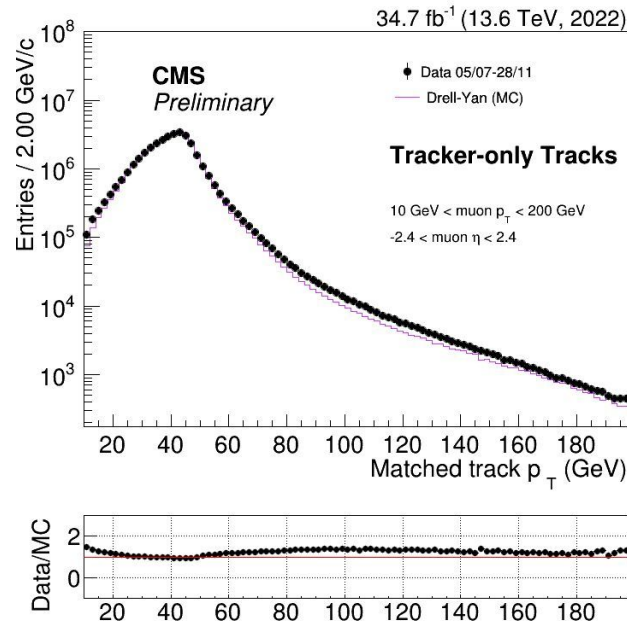


Figure (1a,1b). The histograms show respectively the transverse momentum and η distributions of the **Tracker-only Seeded-Tracks** candidates which have been matched with passing standalone muon probes in 2022 analysis both for Data (black dots) and MC (violet line). The uncertainties shown are statistical and are frequently smaller than the marker size. The agreement between data and MC becomes of 1-2% when probe kinematic properties are far from the lower and upper bounds settings in the η distribution, and when the DY more sensitive region [25,60] GeV gets closer in transverse momentum distribution. Very similar behavior has been observed for **all Tracks** collection tracks.

Matching inefficiency

To estimate the matching inefficiency $1 - \epsilon_M$, the three most influential passing probe matching selection distributions (ΔR , $\Delta\eta$ and $\Delta p_T/p_T(\text{probe})$) in **all Tracks** collection have been plotted up to the thresholds described on page 4 for the ranges of pseudorapidity η [-2.4,2.4] and p_T [10,200] GeV of probe standalone muons. The estimate of $1 - \epsilon_M$ is taken as a sum of fraction of the upper 20% (along x) in each distribution. Additionally, the same estimate was obtained for the outermost bins in absolute pseudorapidity η [2.1,2.4] and transverse momentum p_T [120,200] GeV of probe standalone muons where the matching distributions were found to be more broad. The estimates for 2022 sample are summarized in the table below. Different colors have been used to visually distinguish their ranges.

34.7 fb ⁻¹ (13.6 TeV, 2022) All Tracks	ΔR	$\Delta\eta$	$\Delta p_T/p_T(\text{probe})$	Sum of contributions for $1 - \epsilon_M$
$1 - \epsilon_M$ (Data) [%] η in [-2.4,2.4] and p_T in [10,200] GeV	<0.01	<0.01	<0.06	<0.1
$1 - \epsilon_M$ (DY MC) [%] η in [-2.4,2.4] and p_T in [10,200] GeV	<0.01	<0.01	<0.03	<0.1
$1 - \epsilon_M$ (Data) [%] Upper bound for $ \eta $ in [2.1,2.4]	<0.01	<0.01	<0.1	<0.11
$1 - \epsilon_M$ (DY MC) [%] Upper bound for $ \eta $ in [2.1,2.4]	<0.01	<0.01	<0.31	<0.32
$1 - \epsilon_M$ (Data) [%] Upper bound for p_T in [120,200] GeV	<0.01	<0.01	<2.9	<3.0
$1 - \epsilon_M$ (DY MC) [%] Upper bound for p_T in [120,200] GeV	<0.01	<0.01	<4.7	<4.8

2022 Fake matching rate

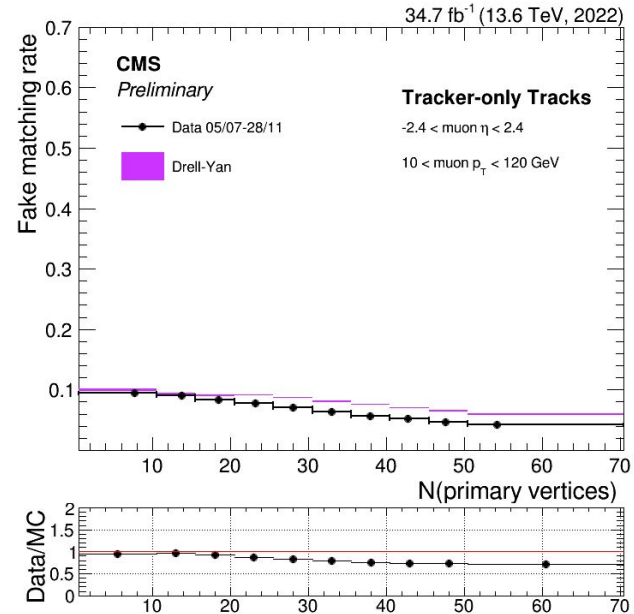
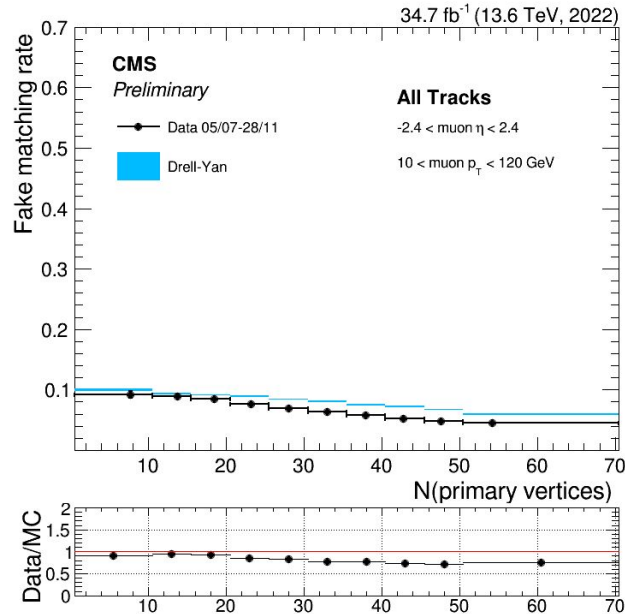


Figure 1a,1b. The fake matching rate ϵ_F in the **All Tracks** and **Tracker-only seeded tracks** collections as a function of **number of primary vertices**. Data (black dots) and Madgraph DY (light blue and violet rectangles). The uncertainties shown are statistical and are frequently smaller than the marker size. Systematic uncertainties related to fit functions, geometrical acceptance gaps and matching probability can be significant. Agreement between data and MC stays within 30%. As described in page 5, the application of ϵ_F to estimate ϵ_T reduces the measured inefficiency fractionally by less than 10% for both **All Tracks** and **Tracker-only seeded tracks** collections to obtain the true inefficiency estimate. As pileup increases, tracks combining with tags near Z boson mass (40-200 GeV) increases. By removing these tracks, the remaining tracks sample has fewer potential fake matches, leading to a lower fake matching rate overall.

The gen truth study

Since the usage of fit procedure in Tag and Probe can introduce significant systematics uncertainties, the performance results from traditional fit procedure strategy have been compared with a generator truth efficiency computation on MC passing through the following steps:

1. Find **generator level muon particles** from hard process
2. Require **two opposite charge muons** from the same Z boson mother
3. Apply same tag and probe **selection strategy of reconstructed muon candidates** (page 6)
4. Matching probe-track candidates procedure (page 6) is applied to the **subleading transverse momentum generator** level muon (probe). Note that a mismatch during gen matching can affect the measurement
5. Cleaning of tag-probe pairs (page 3)
6. Average matching outcome on each kinematic variables bin, with no PU reweighting

The study is presented for **2022**, **2023** and **2023postBPix** proton-proton data sample.

2022 Tracking performance

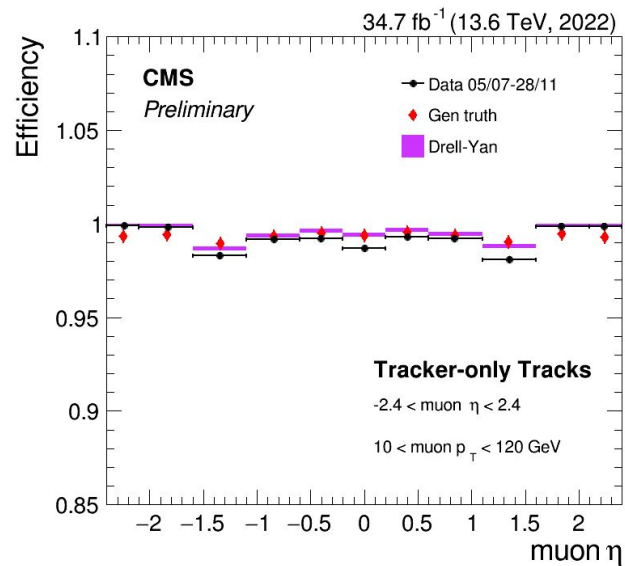
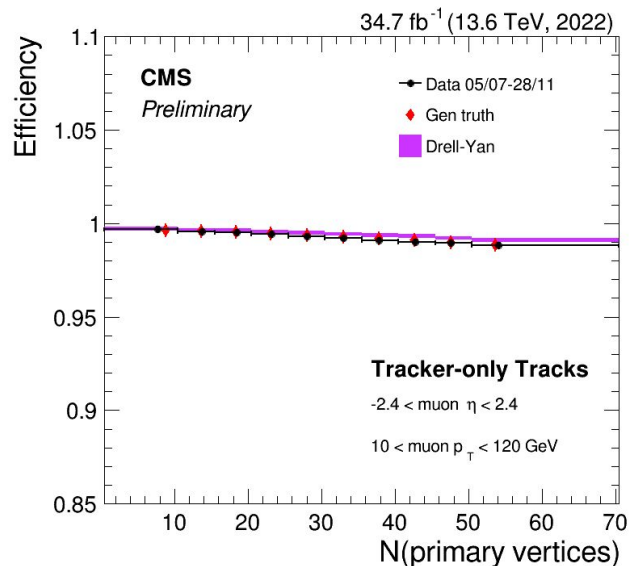


Figure a,b,c. The tracking efficiency in the **Tracker-only seeded tracks** collection as a function of **number of primary vertices** and **pseudorapidity η** of probe standalone muons. Data (black dots) and Madgraph DY (violet rectangles). Gen truth study is shown in red diamonds. The uncertainties shown includes statistical and matching probability contributions and are frequently smaller than the marker size. Systematic uncertainties related to fit functions, geometrical acceptance gaps can be significant. The different methods are showing the range of systematics. Agreement between data and MC stays within 1%. The biggest disagreement between data and MC is observed in the transition between the barrel and end-cap region.

2022 Tracking performance

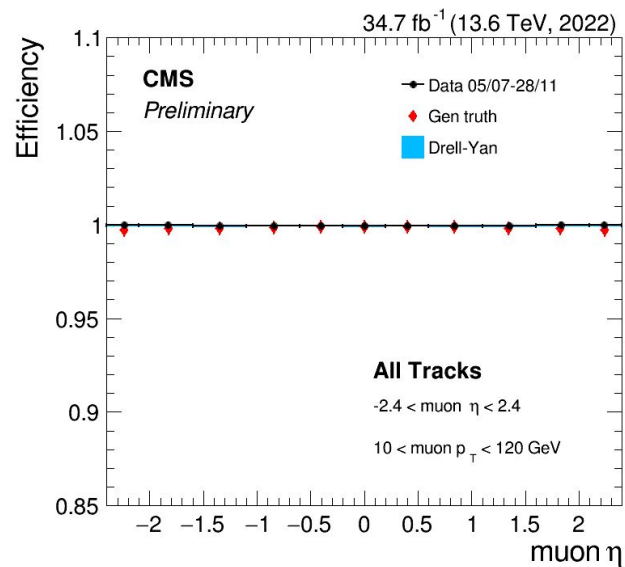
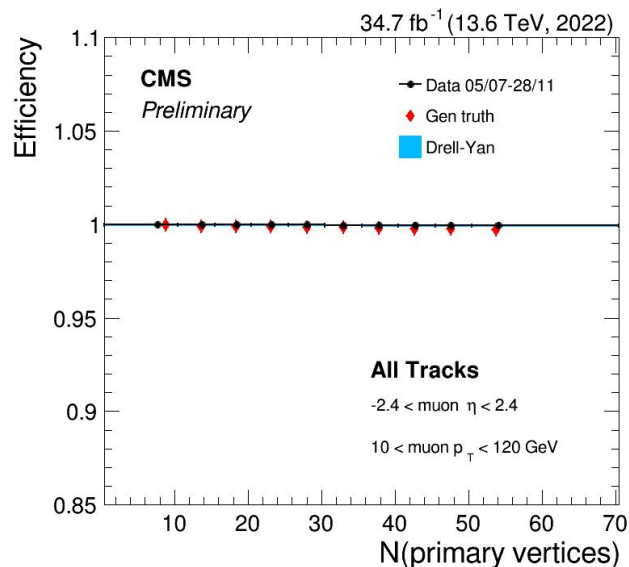


Figure a,b,c. The tracking efficiency in the **All Tracks** collection as a function of **number of primary vertices** and **pseudorapidity η** of probe standalone muons. Data (black dots) and Madgraph DY (light blue rectangles). Gen truth study is shown in red diamonds. The uncertainties shown includes statistical and matching probability contributions and are frequently smaller than the marker size. Systematic uncertainties related to fit functions, geometrical acceptance gaps can be significant. The different methods are showing the range of systematics. Agreement between data and MC stays within 0.3%. As expected, the **last two iterations** involving **signals from muon systems** help to improve considerably the muon reconstruction efficiency.

2022 Tracking performance

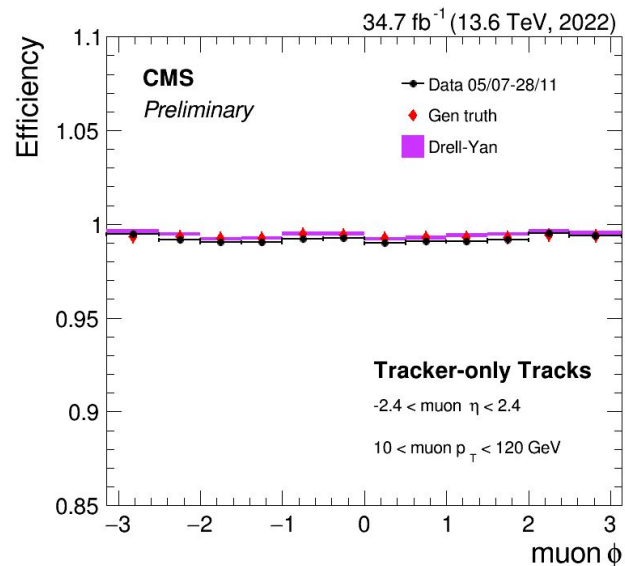
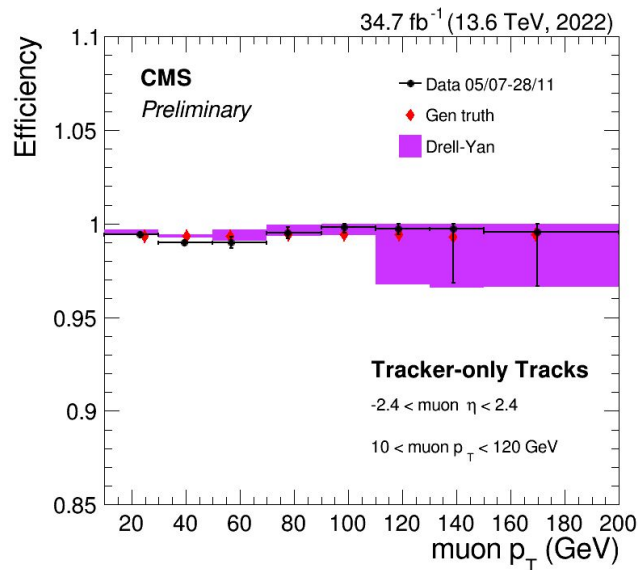


Figure a,b,c. The tracking efficiency in the **Tracker-only seeded tracks** collection as a function of **transverse momentum p_T** and **azimuthal angle ϕ** of probe standalone muons. Data (black dots) and Madgraph DY (violet rectangles). Gen truth study is shown in red diamonds. The uncertainties shown includes statistical and matching probability contributions. Systematic uncertainties related to fit functions, geometrical acceptance gaps can be significant. The different methods are showing the range of systematics. Agreement between data and MC stays within 1%.

2022 Tracking performance

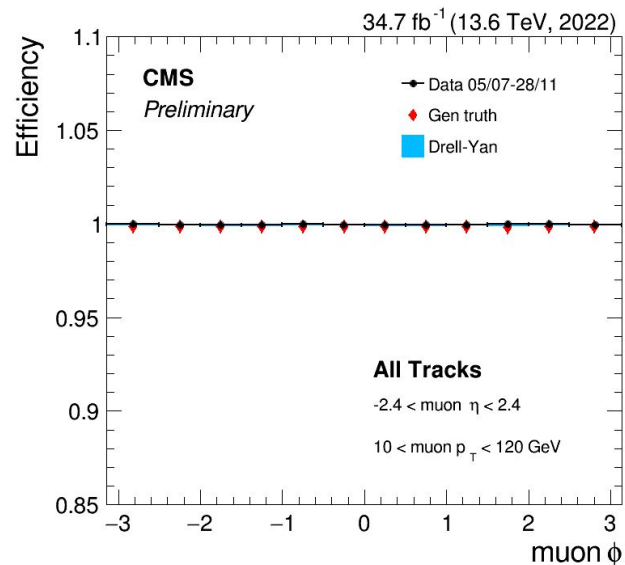
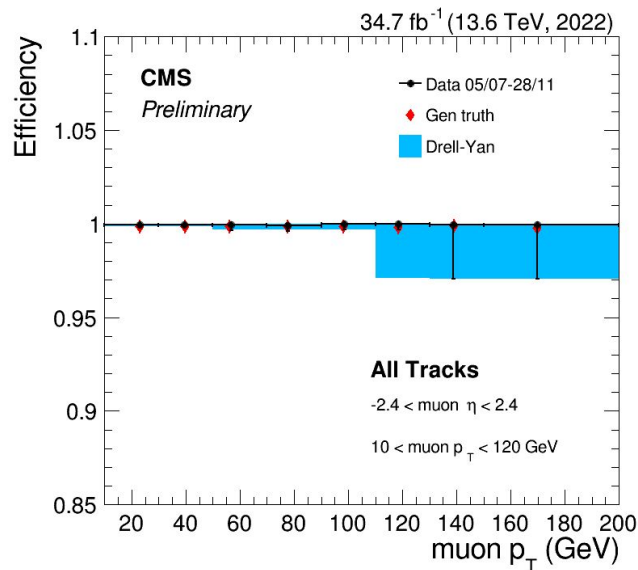


Figure a,b,c. The tracking efficiency in the **All Tracks** collection as a function of **transverse momentum p_T** and **azimuthal angle ϕ** of probe standalone muons. Data (black dots) and Madgraph DY (light blue rectangles). Gen truth study is shown in red diamonds. The uncertainties shown includes statistical and matching probability contributions and are frequently smaller than the marker size. Systematic uncertainties related to fit functions, geometrical acceptance gaps can be significant. The different methods are showing the range of systematics. Agreement between data and MC stays within 1%. As expected, the **last two iterations** involving **signals from muon systems** help to improve considerably the muon reconstruction efficiency.

2023 Tracking performance

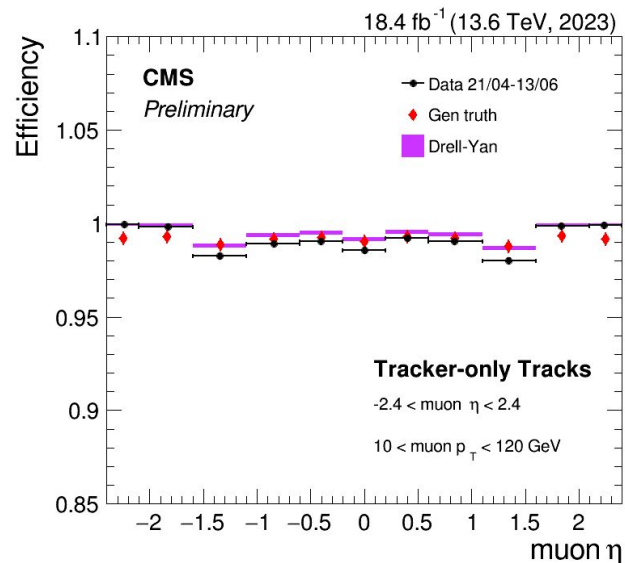
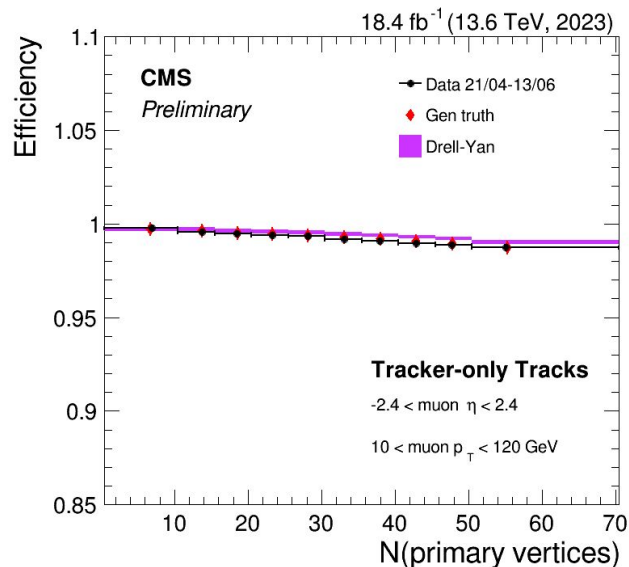


Figure a,b,c. The tracking efficiency in the **Tracker-only seeded tracks** collection as a function of **number of primary vertices** and **pseudorapidity η** of probe standalone muons. Data (black dots) and Madgraph DY (violet rectangles). Gen truth study is shown in red diamonds. The uncertainties shown includes statistical and matching probability contributions and are frequently smaller than the marker size. Systematic uncertainties related to fit functions, geometrical acceptance gaps can be significant. The different methods are showing the range of systematics. Agreement between data and MC stays within 1%. The biggest disagreement between data and MC is observed in the transition between the barrel and end-cap region.

2023 Tracking performance

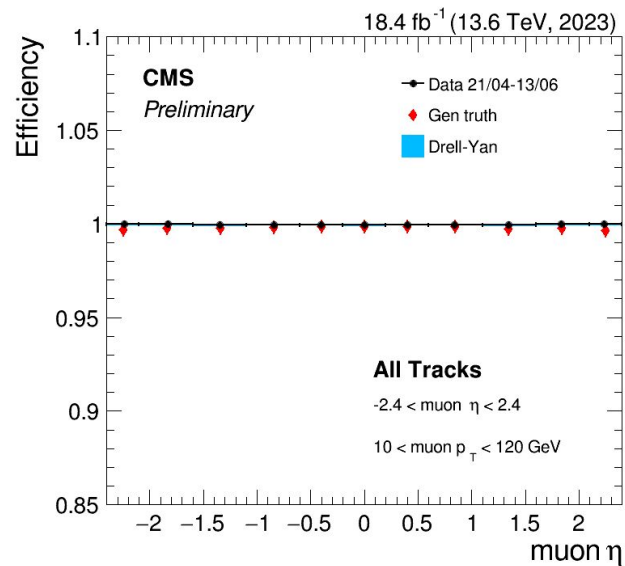
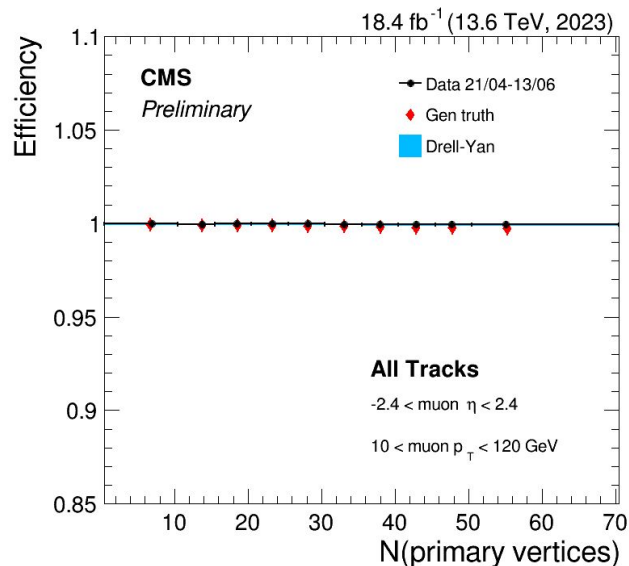


Figure a,b,c. The tracking efficiency in the **All Tracks** collection as a function of **number of primary vertices** and **pseudorapidity η** of probe standalone muons. Data (black dots) and Madgraph DY (light blue rectangles). Gen truth study is shown in red diamonds. The uncertainties shown includes statistical and matching probability contributions and are frequently smaller than the marker size. Systematic uncertainties related to fit functions, geometrical acceptance gaps can be significant. The different methods are showing the range of systematics. Agreement between data and MC stays within 0.3%. As expected, the **last two iterations** involving **signals from muon systems** help to improve considerably the muon reconstruction efficiency.

2023 Tracking performance

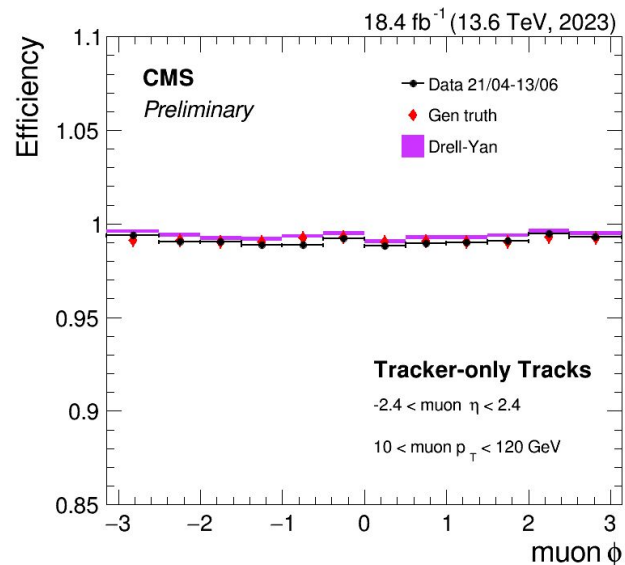
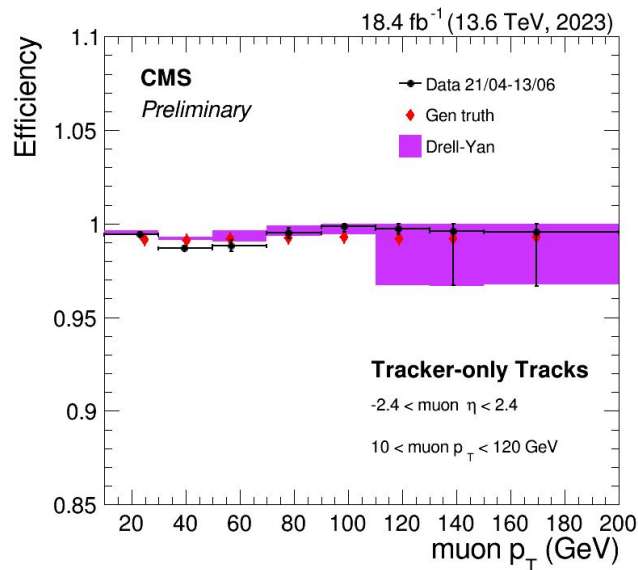


Figure a,b,c. The tracking efficiency in the **Tracker-only seeded tracks** collection as a function of **transverse momentum p_T** and **azimuthal angle ϕ** of probe standalone muons. Data (black dots) and Madgraph DY (violet rectangles). Gen truth study is shown in red diamonds. The uncertainties shown includes statistical and matching probability contributions and are frequently smaller than the marker size. Systematic uncertainties related to fit functions, geometrical acceptance gaps can be significant. The different methods are showing the range of systematics. Agreement between data and MC stays within 1%.

2023 Tracking performance

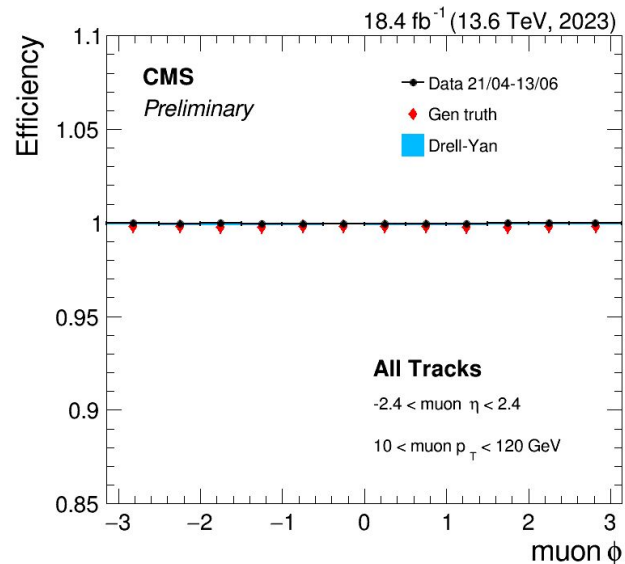
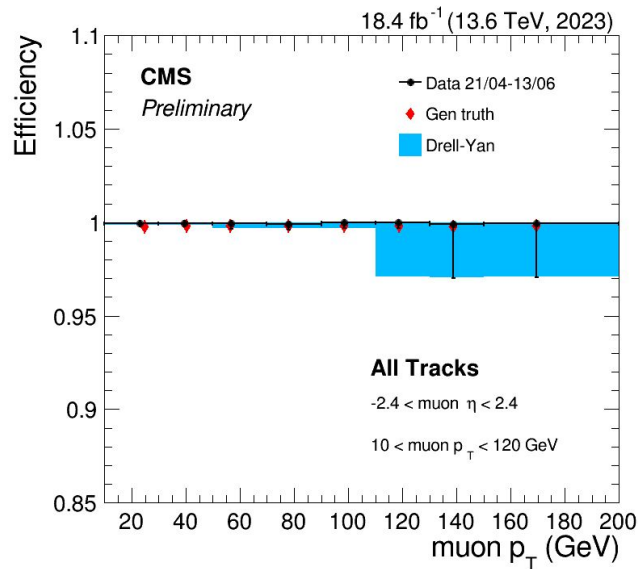


Figure a,b,c. The tracking efficiency in the **All Tracks** collection as a function of **transverse momentum p_T** and **azimuthal angle ϕ** of probe standalone muons. Data (black dots) and Madgraph DY (light blue rectangles). Gen truth study is shown in red diamonds. The uncertainties shown includes statistical and matching probability contributions and are frequently smaller than the marker size. Systematic uncertainties related to fit functions, geometrical acceptance gaps can be significant. The different methods are showing the range of systematics. Agreement between data and MC stays within 1%. As expected, the **last two iterations** involving **signals from muon systems** help to improve considerably the muon reconstruction efficiency.

2023postBPix Tracking performance

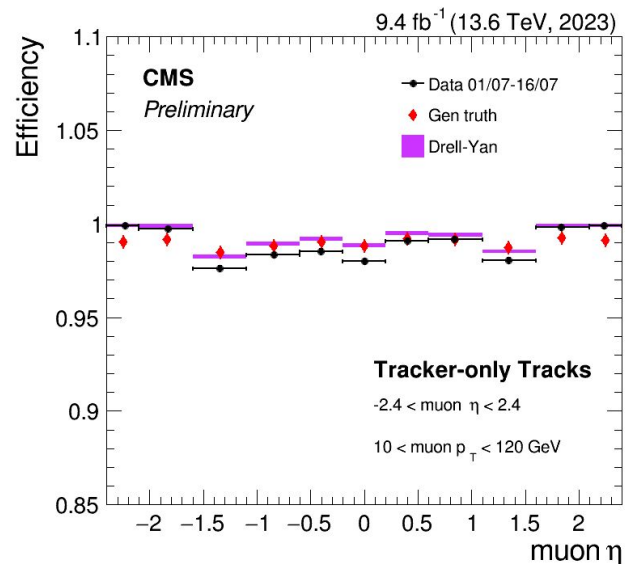
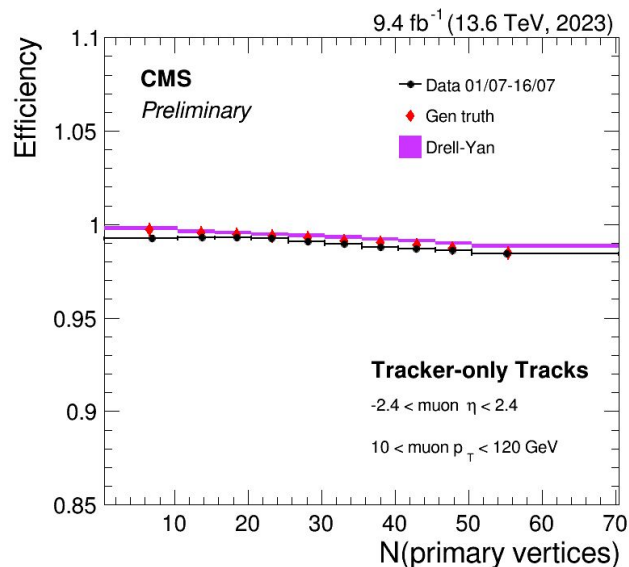


Figure a,b,c. The tracking efficiency in the **Tracker-only seeded tracks** collection as a function of **number of primary vertices** and **pseudorapidity η** of probe standalone muons. Data (black dots) and Madgraph DY (violet rectangles). Gen truth study is shown in red diamonds. The uncertainties shown includes statistical and matching probability contributions and are frequently smaller than the marker size. Systematic uncertainties related to fit functions, geometrical acceptance gaps can be significant. The different methods are showing the range of systematics. Agreement between data and MC stays within 1%. The biggest disagreement between data and MC is observed in the transition between the barrel and end-cap region.

2023postBPix Tracking performance

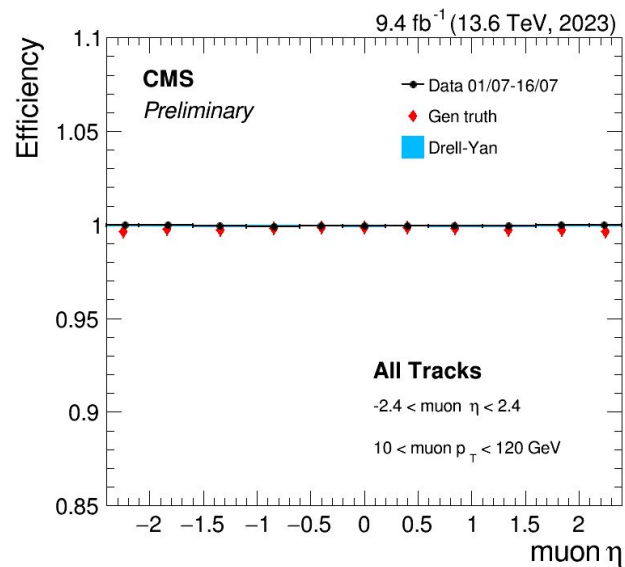
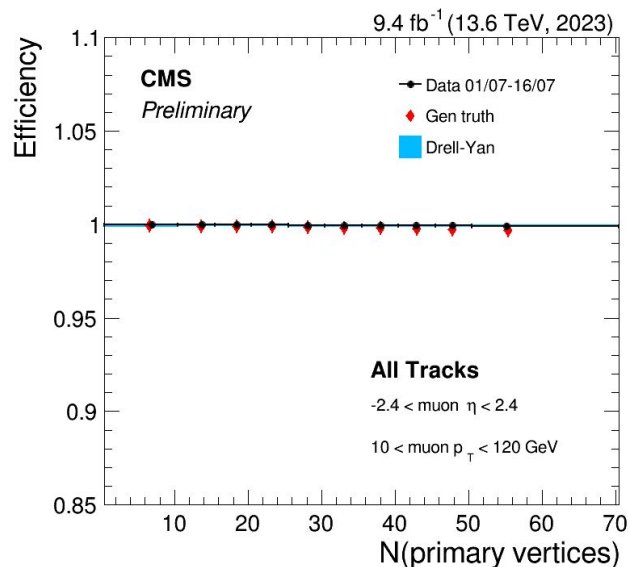


Figure a,b,c. The tracking efficiency in the **All Tracks** collection as a function of **number of primary vertices** and **pseudorapidity η** of probe standalone muons. Data (black dots) and Madgraph DY (light blue rectangles). Gen truth study is shown in red diamonds. The uncertainties shown includes statistical and matching probability contributions and are frequently smaller than the marker size. Systematic uncertainties related to fit functions, geometrical acceptance gaps can be significant. The different methods are showing the range of systematics. Agreement between data and MC stays within 0.3%. As expected, the **last two iterations** involving **signals from muon systems** help to improve considerably the muon reconstruction efficiency, including the problematic region of the pixel tracker ($-1.5 < \eta < -0.2$).

2023postBPix Tracking performance

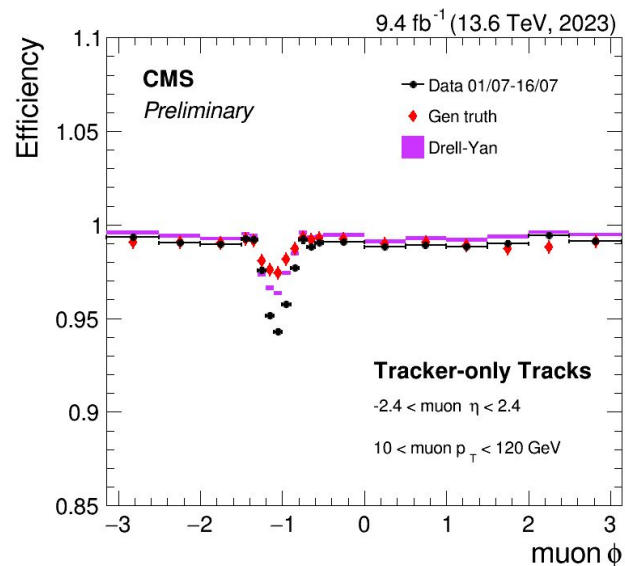
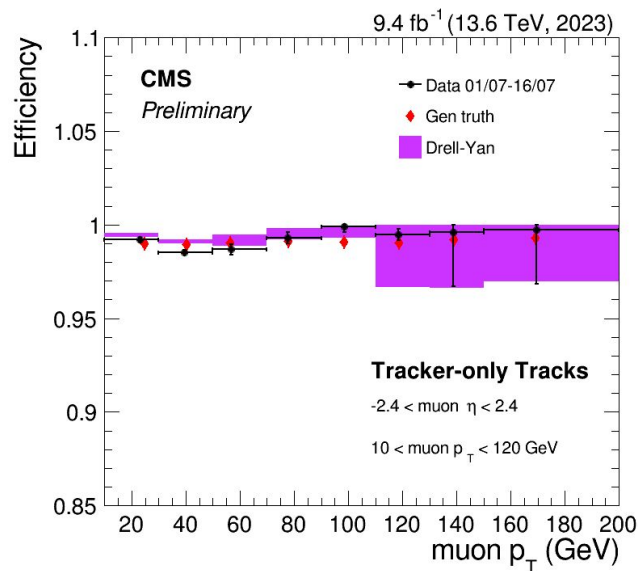


Figure a,b,c. The tracking efficiency in the **Tracker-only seeded tracks** collection as a function of **transverse momentum p_T** and **azimuthal angle ϕ** of probe standalone muons. Data (black dots) and Madgraph DY (violet rectangles). Gen truth study is shown in red diamonds. The uncertainties shown includes statistical and matching probability contributions and are frequently smaller than the marker size. Systematic uncertainties related to fit functions, geometrical acceptance gaps can be significant. The different methods are showing the range of systematics. Agreement between data and MC stays within 1%.

2023postBPix Tracking performance

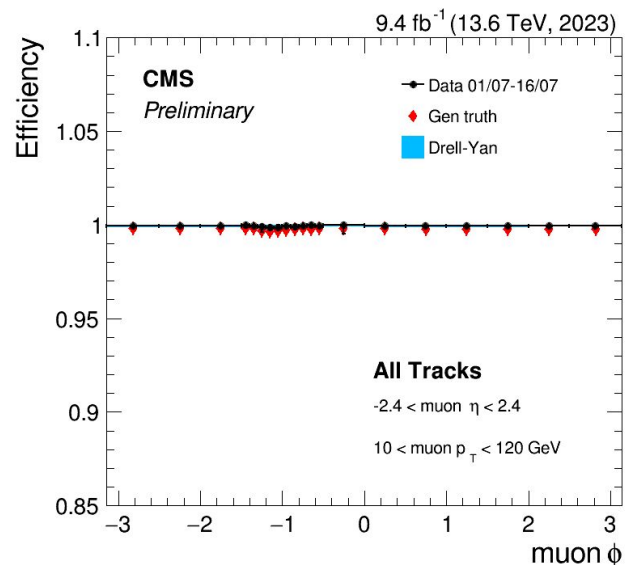
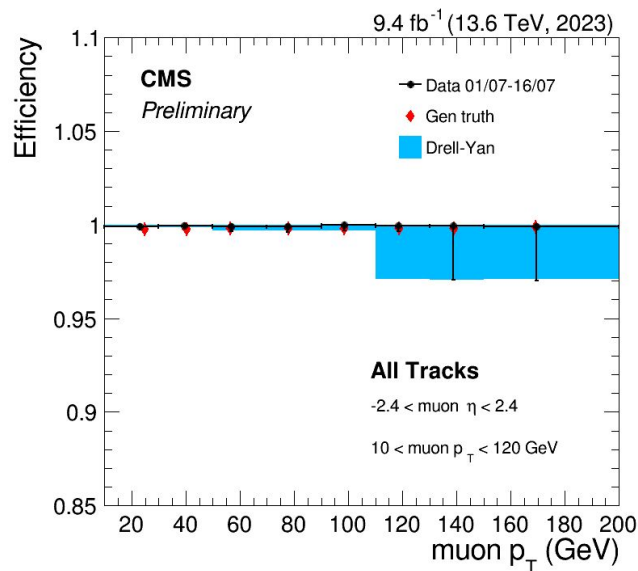


Figure a,b,c. The tracking efficiency in the **All Tracks** collection as a function of **transverse momentum p_T** and **azimuthal angle ϕ** of probe standalone muons. Data (black dots) and Madgraph DY (light blue rectangles). Gen truth study is shown in red diamonds. The uncertainties shown includes statistical and matching probability contributions and are frequently smaller than the marker size. Systematic uncertainties related to fit functions, geometrical acceptance gaps can be significant. The different methods are showing the range of systematics. Agreement between data and MC stays within 1%. As expected, the **last two iterations** involving **signals from muon systems** help to improve considerably the muon reconstruction efficiency, including the problematic region of the pixel tracker ($\phi \sim -1$).

References

- [1] Description and performance of track and primary-vertex reconstruction with the CMS tracker, CMS Collaboration, [TRK-11-001](#), [JINST 9 \(2014\), P10009](#)
- [2] Performance of Run 3 track reconstruction with the mkFit algorithm, CMS Collaboration, [CMS-DP-2022-018](#)
- [3] Documentation of the CMS TagAndProbe package, N. Adam, J. BerryHill, Z. Gecse et al., [CMS Twikipage TagAndProbe \(2010\)](#)
- [4] Performance of the CMS muon detector and muon reconstruction with proton-proton collisions at $\sqrt{s} = 13$ TeV, CMS Collaboration, [JINST 13 \(2018\) no.06, P06015](#)
- [5] Public CMS Data Quality Information, <https://twiki.cern.ch/twiki/bin/view/CMSPublic/DataQuality>
- [6] Operation and performance of the Pixel Detector [CMS-CR-2023-282](#)
- [7] MadGraph5_aMC@NLO, [arXiv:1405.0301 \[hep-ph\]](https://arxiv.org/abs/1405.0301)
- [8] FireWorksWeb, <https://fireworks.cern.ch/>